Mechanistic studies on catalytic alkane oxidation by Murahashi's O2/copper(II)/aldehyde system

Journal:	*Catalysis Science & Technology*
Manuscript ID	CY-ART-07-2023-000944.R1
Article Type:	Paper
Date Submitted by the Author:	18-Jul-2023
Complete List of Authors:	Yamaguchi, Kohei; Osaka University, Department of Applied Chemistry Uemura, Yuya; Osaka University, Department of Applied Chemistry Sugimoto, Hideki; Osaka University, Department of Applied Chemistry Ito, Rin; Osaka University, Department of Applied Chemistry Morimoto, Yuma; Osaka University, Department of Applied Chemistry Itoh, Shinobu; Osaka University, Department of Applied Chemistry;

ARTICLE

Mechanistic studies on catalytic alkane oxidation by Murahashi's O_2/copper(II)/aldehyde system

Received 00th January 20xx,
Accepted 00th January 20xx

DOI: 10.1039/x0xx00000x

Kohei Yamaguchi,[a] Yuya Uemura,[a] Hideki Sugimoto,[a] Rin Ito,[a] Yuma Morimoto[a] and Shinobu Itoh*[a]

Mechanistic studies on catalytic alkane hydroxylation by the Murahashi's O_2/copper(II)/aldehyde system have been conducted to show that the autoxidation of aldehyde (RCHO) by O_2 generating acyl radical intermediate (RC(O)•) is involved as an initiation step of the catalytic cycle. Generated RC(O)• is trapped by O_2 to give an acylperoxyl radical intermediate RC(O)OO•, which may react with another RCHO to generate an adduct intermediate RC(O)OOC(R)(H)O•. Following O–O bond homolytic cleavage of this intermeemediate will give acyloxyl intermediate RC(O)O• and RCOOH, the former of which acts as a reactive species for hydrogen atom abstraction (HAA) from the alkane substrates ($R^1R^2CH_2$; $R^1$and R^2 are alkyl group or hydrogen atom), giving R^1R^2CH•. Generated R^1R^2CH• reacts with O_2 to generate alkylperoxyl radical intermediate R^1R^2CHOO•, which then undergoes Russel reaction to give R^1R^2CHOH (alcohol) and $R^1R^2C{=}O$ (ketone) in a 1 : 1 ratio as the oxidation products. The acyloxyl intermediate RC(O)O• also reacts with RCHO to give carboxylic acid RC(O)OH and RC(O)•, constructing the catalytic cycle. The roles of copper(II) ion in the above catalytic process is also investigated using a series of copper(II) complexes. Furthermore, the Murahashi's system was adopted to catalytic oxidation of methane.

1. Introduction

Alkanes are abundant chemicals widely distributed in petroleum and natural gas. Selective C–H bond functionalization of inert alkane substrates is of great importance for converting them into value-added and easily usable organic compounds.[1,2] In particular, selective oxidation of methane, the main component of natural gas and shale gas as well as methane hydrate, into C1 oxygenates such as methanol, formaldehyde and formic acid has been attracting much recent attention in industrial chemistry.[3-8] Therefore, the development of selective oxidation of alkanes including gaseous alkanes has become an important research topic in industrial chemistry as well as in synthetic organic chemistry.[9,10]

Selective oxidation of organic compounds with molecular oxygen (O_2) is one of the most economically and environmentally desirable reaction, since O_2 is abundant and clean oxidant generating no toxic by-products.[10,11] In this respect, the Murahashi's alkane oxidation reaction using O_2 as an oxidant, copper(II) acetate ($Cu(OAc)_2$) as a catalyst, and acetaldehyde as a sacrificial reductant is an attractive reaction system, where high conversion of alkanes to alcohols and ketones was achieved (Scheme 1).[12-14] Such an O_2/transition-metal/aldehyde catalytic system has also been adopted in *alkene epoxidation* reaction, so-called Mukaiyama epoxidation, where peracids (RC(O)OOH) and/or acyl peroxyl radicals (RC(O)OO•) produced by aldehyde-autoxidation were proposed as the reactive oxidant.[15-19] However, mechanistic details of the Murahashi's alkane oxidation reaction has yet to be clarified.

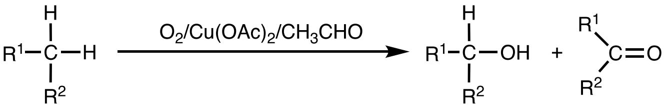

Scheme 1 Murahashi's alkane oxidation reaction

In this study, we have conducted detailed mechanistic studies on the Murahashi's alkane oxidation reaction to get insights into the reactive oxidant as well as the catalytic role of metal ion using a series of Cu^{II}-complexes. Furthermore, the catalytic system was adopted to oxidation of methane.

2. Results and discussion

2.1. Catalytic alkane oxidation with O_2/complex 1/PhCHO system

---

[a] *Department of Molecular Chemistry, Division of Applied Chemistry, Graduate School of Engineering, Osaka University, 2-1 Yamadaoka, Suita, Osaka 565-0871, Japan.*

† Footnotes relating to the title and/or authors should appear here.

Electronic Supplementary Information (ESI) available: [details of any supplementary information available should be included here]. See DOI: 10.1039/x0xx00000x

Murahashi and co-workers reported an efficient alkane oxidation reaction in the presence of acetaldehyde using $Cu(OAc)_2$ as a catalyst (Scheme 1).[12] In this study, we revisited this reaction system to get mechanistic insights into the catalytic alkane oxidation reaction. First, we examined the catalytic oxidation of cyclohexane (CyH) by using $[Cu^{II}(Me_6tren)(CH_3CN)](ClO_4)_2$ (**1**, Me_6tren = tris[2-(dimethylamino)ethyl]amine, see Fig. 1) and benzaldehyde (PhCHO) instead of $Cu(OAc)_2$ and acetaldehyde, respectively. Adoption of the copper(II) complexes enables us to tune the geometry and redox potential of the copper catalyst and the usage of PhCHO allows us to detect the products derived from the aldehyde.

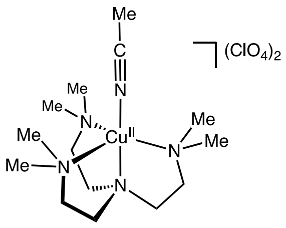

1 (–0.51 V)

Fig. 1 Structure of complex **1.** Reduction potential of **1** (vs. Fc/Fc^+ in acetonitrile) is shown in parentheses. The cyclic voltammogram of **1** is presented in Fig. S2.

The reaction was started by adding PhCHO (0.2 M) to a CH_3CN/CH_2Cl_2 (v/v =3/2) mixed solvent solution containing CyH (2.0 M) and a catalytic amount of **1** (0.2 mM) at 40°C under O_2 atmosphere (Table. 1).

Table 1 Oxidation of cyclohexane (CyH) by the O_2/**1**/PhCHO system

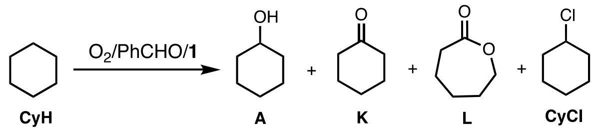

Time/h	Yield/mM				
	A	K	L	CyCl	PhH
1	4.0	2.6	0	0.1	0.7
2	9.8	7.8	0.2	0.5	2.3
3	11	9.5	0.4	0.6	2.9
4	15	15	1.2	0.8	3.2
5	17	16	1.2	1.5	5.2

Reaction condition: [**1**] = 0.2 mM, [PhCHO] = 0.2 M, [Cyclohexane] = 2.0 M in CH_3CN/CH_2Cl_2 (v/v =3/2) at 40 °C under O_2. 51 mM of benzoic acid ($PhCO_2H$) was obtained after 5 h.

Table 1 shows a time-dependent formation of cyclohexanol (**A**), cyclohexanone (**K**), *ε*-caprolactone (**L**) and chlorocyclohexane (CyCl) monitored by GC-FID. **L** may be generated from **K** via Baeyer-Villiger oxidation by perbenzoic acid, PhC(O)OOH (see below discussion). In this reaction, benzene (PhH) was also obtained. Formation of PhH and CyCl suggests involvement of benzoyloxyl radical (PhC(O)O•) and cyclohexyl radical (Cy•) intermediates, respectively (also see below).

To confirm the formation of cyclohexyl radical (Cy•) intermediate, the reaction was carried out in a CH_3CN/CCl_4 mixed solvent (v/v = 3/2) instead of CH_3CN/CH_2Cl_2. As seen in Table S1, the formation ratio of CyCl increased from 3 % to 17 %, clearly demonstrating the formation of Cy•, since CCl_4 has been demonstrated to act as an organic radical trapping agent to give the chlorinated product CyCl.[20]

From the early stage of catalytic reaction (1 h), **A** and **K** were formed in almost 1 : 1 ratio and this ratio was maintained during the reaction as shown in Table 1. If **K** was formed via over-oxidation of **A**, **A** should be the main product at the initial stage of the reaction, and the ratio of **K** should increase gradually afterwards. Thus, the results indicate that the reaction involves "Russell Rearrangement" of tetroxide intermediate (Cy–O–O–O–O–Cy) as shown in Scheme 2.[21] Namely, cyclohexyl radical intermediate (Cy•) formed by hydrogen atom abstraction (HAA) from CyH by a reactive oxidant, rapidly reacts with O_2 at a rate of 10^9 M^{-1} s^{-1} to produce the cyclohexyl-peroxyl radical species (CyOO•).[22] Radical coupling of two CyOO• produces the tetroxide intermediate Cy–O–O–O–O–Cy, from which Russel Rearrangement takes place to give an equal amount of **A** and **K** (Scheme 2). The fact that the amount of **A** slightly exceeded that of **K** in the early stages of the reaction suggests that **A** is also formed directly via the reaction of Cy• and an oxidant such as perbenzoic acid.

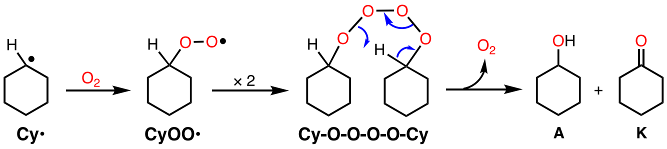

Scheme 2 Russell Rearrangement

The product distribution pattern was almost the same when the reaction mixture was quenched by PPh_3 (Table S2). Since alkylhydroperoxides (ROOH) are known to be quantitatively converted to the corresponding alcohols (ROH) by the reaction with PPh_3,[23] the result indicates that most of CyOO• was converted to the tetroxide intermediate but not to cyclohexyl hydroperoxide (CyOOH).

To get information about the active oxidant, the oxidation reaction of adamantane (AdH) was also examined (Table 2). Oxidation of AdH with **1** and PhCHO under O_2 also proceeded efficiently to give the corresponding alcohols (**3-A** and **2-A**) together with a small amount of ketone (**2-K**). It should be noted that the regioselectivity between the secondary and the tertiary carbons was quite high (3°/2° = 12), suggesting that the active intermediate is not free hydroxy radical (•OH), since Fenton-type autoxidation reaction containing •OH as a reactive oxidant is known to exhibit almost no regioselectivity (3°/2° ~ 1).[24]

Table 2 Oxidation of adamantane (AdH) by the O_2/**1**/PhCHO system

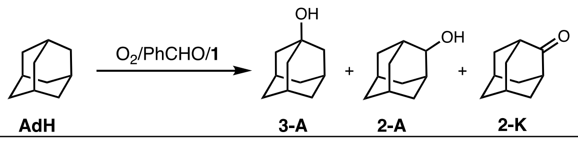

Substrate	Yield/mM ^{a}			3°/2° ^{b}
	3-A	**2-K**	**2-K**	
Adamantane	16	1.7	2.2	12

Reaction conditions: [**1**] = 0.2 mM, [PhCHO] = 0.2 M, [Adamantane] = 0.25 M in CH_3CN/CH_2Cl_2 (*v/v* =3/2) at 40 ºC under O_2. ^{a} The amounts of the products are determined by GC-FID using calibration curves of the products. ^{b} [**3-A**]/([**2-A**] + [**2-K**]) multiplied by 3.

2.2. Reactive oxidant

To explore the reactive oxidants, we focused on the autoxidation of aldehyde. In Scheme 3 is shown a possible mechanism of autoxidation of PhCHO.[25-29] First of all, acyl radical intermediate **a** (PhCO•) is produced by a certain initiating step, which is converted to acyl peroxyl radical intermediate **b** (PhC(O)OO•) by the reaction with O_2. Then, generated acyl peroxyl radical intermediate **b** abstracts hydrogen atom from another molecule of PhCHO, resulting in formation of peracid **d** (PhC(O)OOH) and **a** constructing a radical chain cycle. On the other hand, Hutchings and co-workers recently reported that acyloxyl radical intermediate **c** (PhC(O)O•) is formed through radical adduct formation between **b** and PhCHO and following fragmentation (Scheme 3).[30] Judging from the bond dissociation energy (BDE) of the C–H bond of benzaldehyde (Ph(O)**C–H**, 88.7 ± 2.6 kcal/mol), the O–H bond of perbenzoic acid (PhC(O)O**O–H**, 96.5 kcal/mol), and the O–H bond of benzoic acid (PhC(O)**O–H**, 111 ± 4),[31] acyloxy radicals **c** is the most plausible reactive oxidant for the C–H bond activation of cyclohexane (Cy**–H**, 99.5 kcal/mol).

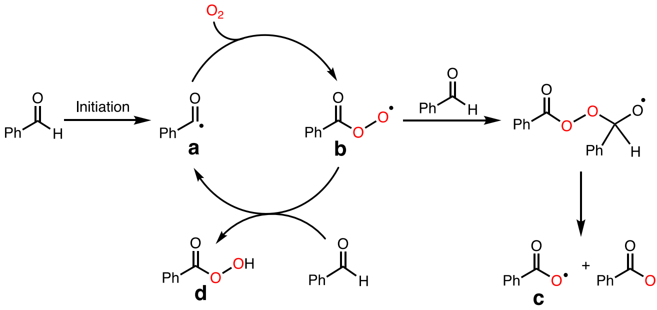

Scheme 3 Autoxidation mechanism of benzaldehyde

It was reported that acyloxy radicals **c** is capable of abstracting hydrogen atom from CyH with a rate constant of about 10^6 M^{-1} s^{-1}.[32] This reaction competes with decarboxylation from **c** with a rate constant of 10^6 s^{-1} to give benzene (PhH) (Scheme 4).[32] Thus, the ratio of the oxidation products (P = **A** + **K** + **L** + CyCl) against benzene (PhH, decarboxylation product of **c**), [P]/[PhH], is expected to increase as the concentration of the substrate increased, since the hydrogen atom abstraction (HAA) process and decarboxylation reaction are competing.

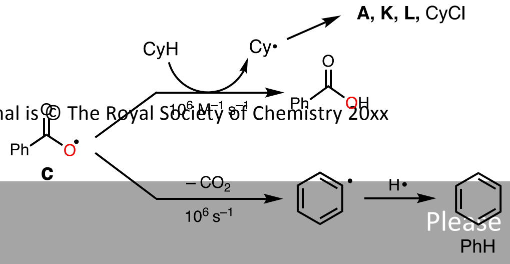

Scheme 4 Competition of HAA with decarboxylation from **c**

As clearly seen in Fig. 2, [P]/[PhH] increased as [CyH] is increased. Thus, we concluded that acyloxy radicals **c** is a reactive oxidant for the HAA from CyH. The amount of benzoic acid ($PhCO_2H$) formed after 5 h was 50 mM, that was larger than the total amount of products (35.7 mM, Table 1). This is reasonable since $PhCO_2H$ is formed both *via* the substrate oxidation by PhC(O)O• (**c**) (Scheme 4) and *via* the autooxidation of PhCHO (Scheme 3).

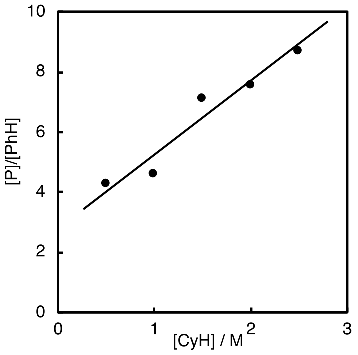

Fig. 2 Dependence of [P]/[PhH] on [CyH]

2.3. Catalytic activity of other Cu^{II}-complexes

In Fig. 3 is compared the catalytic activity of a series of Cu^{II}-complexes **1**–**5** supported by tripodal tetradentate ligands. The crystal structures of them are shown in Fig. S1 together with the crystallographic data in Table S3-S5. Among the Cu^{II}-complexes with similar trigonal bipyramidal structure, complex **1** exhibited the highest initial reaction rate, and the induction period became longer in going from **1** to **5**. These results suggest that the Cu^{II}-complexes play an important role in the alkane oxidation reaction.

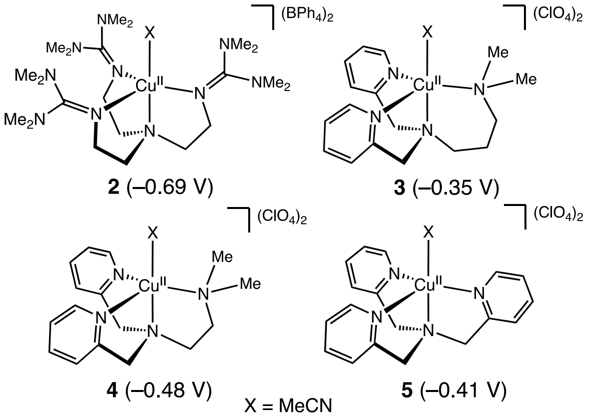

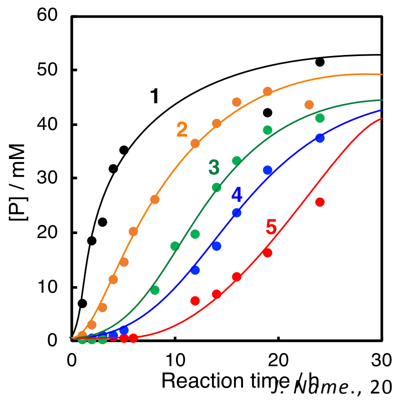

Fig. 3 Time courses of product formation in the oxidation of cyclohexane (2.0 M) catalysed by Cu^{II}-complexes (**1**–**5**, 0.2 mM) with PhCHO (0.2 M) in CH_3CN/CH_2Cl_2 (*v/v* =3/2) at 40°C under O_2. [P] = [**A**] + [**K**] + [**L**] + [CyCl]. Reduction potentials of the Cu^{II}-complexes (vs. Fc/Fc^+ in acetonitrile) are shown in parentheses. The cyclic voltammograms of the Cu^{II}-complexes are presented in Fig. S2.

2.4. Possible role of Cu^{II}-complexes in the Initiation step of aldehyde autoxidation

Generation of acyl radical intermediates **a** (Scheme 3) by the reaction of aldehydes and transition-metal complexes has been proposed as the initiation step of aldehyde autoxidation reactions.[33-35] However, little has been examined on the direct reaction between aldehydes and transition-metal complexes.[36,37] To evaluate such a possibility, we tried to trap acyl radical intermediates **a** in CCl_4 (Table S6). Thus, the reaction of complex **1** (2 mM) with an excess amount of PhCHO (0.2 M) was examined in CCl_4 under an anaerobic condition (to prevent the reaction of **a** with O_2) and then the resulting reaction mixture was poured into methanol. If acyl radical **a** was generated by the reaction of PhCHO and **1**, **a** would be trapped by CCl_4 to generate acyl chloride (PhC(O)Cl),[36,38] which will be converted to methyl benzoate (PhC(O)OMe), more easily detectable product, in methanol (Scheme 5). The same reaction was conducted by using $[Cu^{II}(TEPA)OTf](OTf)$ instead of **1**, since $[Cu^{II}(TEPA)OTf](OTf)$ has much higher reduction potential (+0.05 V vs. Fc/Fc^+) as compared to **1** (–0.51 V). Namely, $[Cu^{II}(TEPA)OTf](OTf)$ is much powerful oxidant than **1**. In both cases, however, no significant difference was observed in the yield of PhC(O)OMe from that of a blank experiment (without the copper complex).

We also tried to trap **a** using acrylonitrile (Fig. S3) or TEMPO (Fig. S4), both of which are known to react with the acyl radical intermediate.[39,40] However, neither the acrylonitrile-adduct **f** nor the TEMPO-adduct **g** were obtained in the presence of complex **1** (Scheme 5).

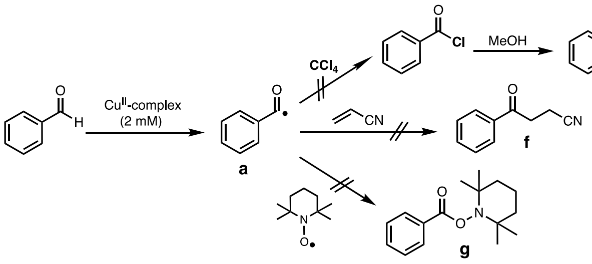

Scheme 5 Acyl radical trapping experiments

Furthermore, if the reaction had played a significant role in the initiation step, the length of the induction period in the catalytic oxidation should have a negative correlation with the redox potential of the Cu^{II}-complexes. However, no such correlation was observed (Fig. 3).

All these results strongly suggest that the direct oxidation of benzaldehyde by the Cu^{II}-complex to generate acyl radical intermediate **a** is negligible under the reaction conditions examined in this study.

2.5. Role of Cu^{II}-complexes in peracid activation

In the oxidation of CyH (2.0 M) with PhCHO (0.2 M) and copper(II) complex under O_2, distinct induction period was observed in the early stage of the reaction (Fig. 3). Even in the case of complex **1** showing the highest initial rate, the induction period became prominent when the concentration of **1** was reduced from 0.2 mM to 0.025 mM (black line in Fig. 4). On the other hand, addition of 10 eq. (based on **1**) of *m*-CPBA (*m*-chloroperbenzoic acid) at the beginning of the reaction significantly shortened the induction period as shown in Fig. 4 (red line), indicating the important role of peracid **d** generated in the catalytic cycle (see Scheme 3).

We assumed that activation of peracid **d** by the Cu^{II}-complex contributes to the shortening of the induction period. To test this possibility, a direct reaction of **1** and *m*-CPBA was examined spectroscopically (Scheme 6). When 10 eq. of *m*-CPBA was added to an acetonitrile solution of **1** (2 mM), the spectrum changed from black (λ_{max} = 845 nm) to red (λ_{max} = 700 nm) in about 30 min at 40°C (Fig. 5A), which was different from the spectrum of the *m*-CBA (*m*-chlorobenzoic acid, decomposition product of *m*-CPBA) adduct of **1** (see Fig. S5). The generated complex exhibited an ESI-mass spectrum showing the peak cluster, whose peak positions as well as isotope distribution pattern are consistent with the chemical formula of an *m*-CPBA adduct complex of **1** (Fig. S6). The *m*-CPBA adduct complex was relatively stable at this temperature, but immediately decomposed when 2,4,6-tri-*tert*-butylphenol (10 equiv) was added to the solution to give 2,4,6-tri-*tert*-butylphenoxyl radical (blue spectrum in Fig. 5B).[58] On the other hand, formation of the phenoxy radical was negligible in the absence of **1**. These results suggest that an adduct formation reaction takes place between the Cu^{II}-complex and peracid **d** generated *in situ* in the catalytic oxidation of CyH by the O_2/Cu^{II}-complex/PhCHO system (Scheme 3).

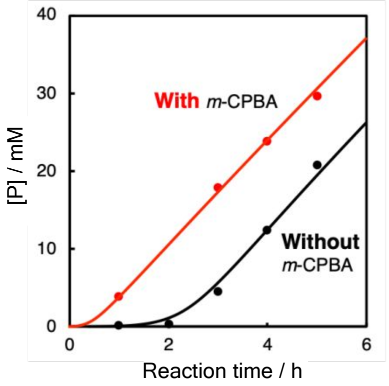

Fig. 4 Time courses of the cyclohexane oxidation by the O_2/**1**/PhCHO system with and without *m*-CPBA (10 mM). Reaction conditions: [**1**] = 0.025 mM, [PhCHO] = 0.2 M, [Cyclohexane] = 2.0 M at 40°C under O_2.

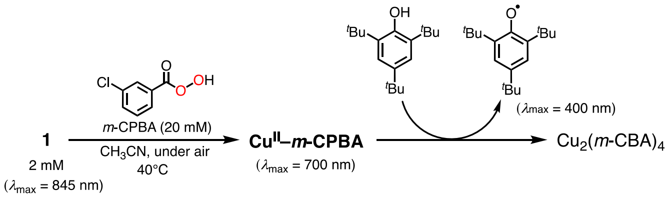

Scheme 6 Reaction of **1** and *m*-CPBA

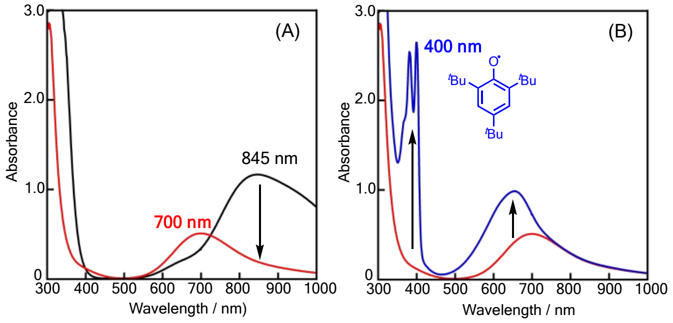

Fig. 5 (A) UV-vis spectral change observed upon an addition of *m*-CPBA (10 eq.) to **1** (2 mM) at 40°C in acetonitrile and (B) UV-vis spectral change of the reaction between the *m*-CPBA adduct Cu^{II}-complex with 2,4,6-tri-*tert*-butylphenol (10 eq.).

To further investigate the role of Cu^{II}-complexes in the peracid activation process, the catalytic oxidation of CyH was performed under anaerobic (N_2) conditions in the presence of **1** and *m*-CPBA. When the catalytic oxidation of CyH (2.0 M) by *m*-CPBA (0.2 M) was carried out in the presence of a catalytic amount of **1** (0.2 mM) in a CH_3CN/CH_2Cl_2 (*v*/*v* = 3/2) mixed solvent, **A** was obtained as the major product together with **K**, **L** and **CyCl** as the minor products (Fig. S7). The catalytic activity of the Cu^{II}-complexes **2**–**5** was also examined under the same conditions (Fig. S7). Apparently, the Cu^{II}-complexes showed different catalytic activity, which correlates with the length of the induction period observed in the O_2/Cu^{II}-complex/PhCHO system except **2** as shown in Fig. 6. Namely, the higher the catalytic activity in the *m*-CPBA system, the shorter the induction period in the O_2/Cu^{II}-complex/PhCHO system. Therefore, it can be concluded that the peracid activation by Cu^{II}-complex accelerates the catalytic reaction of CyH in the early stages of the catalytic reaction. Deviation of complex **2** from the straight line shown in Fig. 6 may be due to steric hindrance of the TMG substituents around the metal center, which prohibits the substrate access to the metal centre. Deactivation of complex **2** by intramolecular hydroxylation of the methyl group of TMG substituents may also cause its lower catalytic activity.[41]

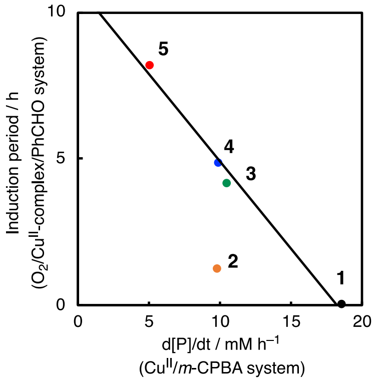

Fig. 6 Correlation between length of the induction period in the O_2/PhCHO/Cu^{II}-complex system and the catalytic activity of Cu^{II}-complexes in the oxidation of cyclohexane by *m*-CPBA.

Given the linear correlation shown in Fig. 6 and that the aldehyde autoxidation produces peracids (Scheme 3), the induction phase in the O_2/Cu^{II}-system/PhCHO is thought to involve formation of a Cu^{II}-peracid complex, which cleaves the C–H bond of PhCHO to generate acyl radical intermediates **a,** accelerating the autooxidation reaction of PhCHO (Scheme 3). To get mechanistic insights into the peracid activation process in the early stages of the catalytic reaction, we further investigated the induction period phase as below.

As shown in Fig. 7 (black line), there was a prominent induction period of about 2 h, when the lower concentration (0.025 mM) of **1** was used as a catalyst. If the reaction started without adding **1** at the beginning and then **1** was added to the reaction solution after 2h, there was almost no induction period after the addition of **1** (Fig. 7, blue line). Namely, **1** was not involved in the induction process (first 2 h). Considering that aldehydes are sensitive to air, the formation of peracids by the oxidation of aldehydes may be the true initiating reaction. Indeed, iodometry revealed that peroxide formation increased with time when PhCHO was stirred in acetonitrile in an O_2 atmosphere under conditions that minimized the influence of metal particles, using aqua regalis rinsed vial and stirrer (Fig. S8). Thus, we concluded that the Cu^{II}-complex play an important role in initiating the aldehyde autoxidation reaction by reacting with the peracid produced by the direct reaction of PhCHO and O_2.

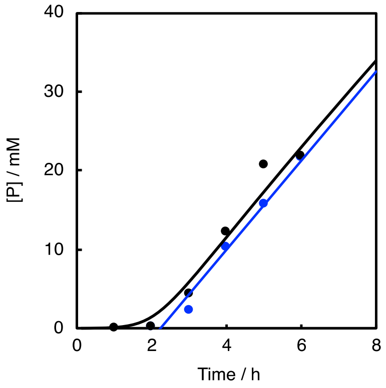

Fig. 7 Time courses of the product formation in the O_2/**1**/PhCHO system (black line) and that of the reaction where **1** was added after 2 h (blue line). Reaction condition: [PhCHO] = 0.2 M, [Cyclohexane] = 2.0 M, $[\mathbf{1}]_0$ = 0.025 mM at 40°C under O_2.

2.6. Application to methane oxidation

Finally, oxidation of methane was briefly examined using the Murahashi's system. In this reaction, $Cu(OAc)_2$ was used as a catalyst to avoid intramolecular and/or intermolecular ligand hydroxylation (catalyst degradation). Thus, the oxidation of methane was carried out in a pressurized condition (CH_4 = 3.0 MPa, O_2 = 1.0 MPa) in the presence of $Cu(OAc)_2$ (0.040 μmol) and PhCHO (2.0 mmol) at ambient temperature (25°C) for 8 h in CH_3CN. GC-MS analysis of the final reaction solution indicated formation of methanol in a 2.0 μmol amount as shown in Fig. S9. Formation of a trace amount of formaldehyde was also noted. The low yield of the oxidation products is apparently due to the higher BDE of methane (105 kcal/mol) compared to that of CyH (98 kcal/mol) and the lower concentration of the gaseous substrate.

3. Conclusions

In this study, we have conducted a mechanistic study on the catalytic alkane oxidation by O_2/Cu^{II}-complex/RCHO system (Murahashi's reaction). The reaction of RCHO and O_2 generates acyl-peroxyl radical RC(O)OO• intermediate **b** via the formation of acyl radical intermediate **a** (Scheme 3). Generated RC(O)OO• (**b**) abstract hydrogen atom from another RCHO to give **a** and peracid **d**, constructing a radical chain cycle. Intermediate **b** also undergoes adduct formation with RCHO to generate RC(O)OOC(O)(H)O• intermediate, from which acyloxyl radical **c** and RC(O)OH are produced. Judging from the high BDE of RC(O)O–H (111 ± 4 kcal/mol), acyloxyl radical **c** is the most powerful oxidant for the hydrogen atom abstraction (HAA) from the alkane substrate (Scheme 4). Then, generated alkane radical intermediate undergoes Russell reaction to give alcohol (**A**) and Ketone (**K**) products (Scheme 2).

Regarding to the role of copper(II) complex, we expected that the higher the oxidation ability of the copper(II) complexes the larger the activation rate of PhCHO, shortening the induction period. However, there was no such correlation between the redox potential of the copper(II) complexes and the length of the induction period (Fig. 3). This is one of the pieces of evidence that the copper(II) complexes do not participate directly to the oxidation of PhCHO to generate acyl radical intermediates **a**. On the other hand, there was a good linear correlation (except complex **2**) between the length of induction period and the catalytic activity of the copper(II) complexes in the *m*-CPBA system (Fig. 6). This result indicates that the activation of peracid by the copper(II) complex is involved in the induction period of the catalytic oxidation. This assumption is consistent with the result shown in Fig. 7. Thus, we concluded that the significant role of the copper(II) complex is the activation of peracid **d** to generate copper(II)-peracid adduct intermediate, which may also generate reactive oxidant to accelerate the autoxidation of RCHO.

Oxidation of methane was briefly examined using the Murahashi's system. Judging from the BDEs (RC(O)O–H: 111 ± 4 kcal/mol vs. H_3C–H: 105 kcal/mol), the presumed reactive oxidant, acyloxyl radical **c**, has an enough power to induce the HAA from methane. However, the available concentration of methane (3.0 MPa) was too low to compete with the oxidation of PhCHO. Nonetheless, the present study will give important information for the development of efficient catalytic system for gaseous alkane oxidation reaction.

4. Experimental section

4.1. General

The reagents and the solvents used in this study, except the ligands and the copper complexes, were commercial products of the highest available purity and were purified by the standard methods,[42] if necessary. *m*-Chloroperbenzoic acid (*m*-CPBA) was purified by recrystallization from CH_2Cl_2 in refrigerator kept at –20°C, and the purity was determined to be 80-90% by redox titration using NaI. Ligands (TMPA,[43] TEPA,[44] Me$_2$-uns-penp,[45] TMG$_3$tren[46] and Me$_2$-pp3[47]) and Cu^{II}-complexes ([Cu^{II}(Me$_6$tren)(CH$_3$CN)](ClO$_4$)$_2$ (**1**),[48] [Cu^{II}(TMPA)(CH$_3$CN)](ClO$_4$)$_2$ (**5**)[49] and [Cu^{II}(TEPA)(OTf)](OTf) (**6**)[50]) were prepared according to the reported procedures. Anaerobic reactions were carried out under N_2 atmosphere using a glovebox (Miwa DB0-1KP or KK-011- AS, KOREA KIYON product, [O_2]<1 ppm). UV-visible spectra were taken on a Jasco V-570 or a Hewlett Packard 8453 photo diode array spectrophotometer equipped with a Unisoku thermostated cryostat cell holder USP-203. Near IR spectra were taken on Jasco V-670. ^{1}H-NMR spectra were recorded on a JEOL ECP400. Elemental analyses were performed on a Yanaco New Science Inc. CHN order MT-5 or a J-SCIENCE LAB Co., Ltd. MICRO CORDER JM10. ESI-MS (electrospray ionization-mass spectrometry) measurements were performed on a BRUKER cryospray microTOFII. Gas chromatography (flame ionization detector) measurements were performed on a Shimadzu GC-2010 equipped with a GL Science InertCapWAX capillary column (30 m×0.25 mm), an AOC-20s auto sampler, and an AOC-20i auto injector. Gas chromatography-mass spectrometry (GC-MS) measurements were performed on a Shimadzu GCMS-QP2010 Plus equipped with a RESTEK Rtx-VMS column (30 m × 0.25 mm), an AOC-20s auto sampler, and an AOC-21i auto injector.

4.2. Synthesis

[Cu^{II}(TMG$_3$tren)(CH$_3$CN)](BPh$_4$)$_2$ (2). An acetonitrile solution (1 mL) of Cu^{II}(ClO$_4$)$_2$•6H$_2$O (73 mg, 0.197 mmol) was added to an acetonitrile solution (1 mL) of TMG$_3$tren (87 mg, 0.197 mmol). The colour of the solution changed from pale blue to green. After stirring the mixture for 5 min, the reaction mixture was treated with 2 eq. of NaBPh$_4$ (135 mg, 0.394 mmol). The reaction mixture was added to an excess amount of Et$_2$O to give pale green precipitate. The resulting solid was collected by filtration and dried under vacuum. Recrystallization from CH$_3$CN/Et$_2$O gave green crystal suitable for X-ray crystallographic analysis: 43 mg, 18 %. ESI-MS (pos): *m/z* = 538.31, calcd. for ([Cu^{II}(TMG$_3$tren)Cl]$^+$) 538.30. Elemental Anal: calcd. for ([Cu^{II}(TMG$_3$tren)(CH$_3$CN)(BPh$_4$)$_2$]) (CuC$_{71}$H$_{91}$N$_{11}$B$_2$): C; 71.80, H; 8.06, N; 12.97. Found: C; 71.79, H; 7.96, N; 13.08.

[Cu^{II}(Me$_2$-pp3)(CH$_3$CN)](ClO$_4$)$_2$ (3). An acetonitrile solution (2.0 mL) of Cu^{II}(ClO$_4$)$_2$•6H$_2$O (324 mg, 0.875 mmol) was added to an acetonitrile solution (1.5 mL) of Me$_2$-pp3 (249 mg, 0.875 mmol). The colour of the solution changed from pale blue to deep blue. After stirring for 5 min, the reaction mixture was added to an excess amount of Et$_2$O to give blue precipitate. The resulting solid was collected by filtration and dried under vacuum. Recrystallization from CH$_3$CN/Et$_2$O gave blue crystal: 86 mg, 17 %. ESI-MS (pos): *m/z* = 382.10, calcd. for ([Cu^{II}(Me$_2$-pp3)Cl]$^+$) 382.10. Elemental Anal: calcd. for ([Cu^{II}(Me$_2$-pp3)(CH$_3$CN)(ClO$_4$)$_2$]) (CuC$_{19}$H$_{27}$N$_5$Cl$_2$O$_8$): C; 38.82, H; 4.63, N; 11.91. Found: C; 38.78, H; 4.70, N; 11.95.

[Cu^{II}(Me$_2$-uns-penp)(CH$_3$CN)](ClO$_4$)$_2$ (4). This compound was prepared by a similar procedure to that for the synthesis of [Cu^{II}(Me$_2$-pp3)(CH$_3$CN)](ClO$_4$)$_2$ (**3**): 41 mg, 20 %. ESI-MS (pos): *m/z* = 368.08, calcd. for ([Cu^{II}(Me2-uns-penp)Cl]$^+$) 368.08.

Elemental Anal: calcd. for ([Cu^{II}(Me_2-uns-penp)(CH_3CN)(ClO_4)$_2$]) ($CuC_{18}H_{25}N_5Cl_2O_8$): C; 37.80, H; 4.37, N; 12.20. Found: C; 37.16, H; 4.31, N; 12.12.

4.3. X-ray crystallographic analysis

Single crystals of the copper(II) complexes were mounted on a DT-MicroLoop (MiTegan, LLC) with mineral oil. Data of X-ray diffraction were collected on a Rigaku R-AXIS RAPID diffractometer using filtered MoKα radiation (λ = 0.71075 Å). A direct method of SHELXT was used for the structure solution of the crystals. All calculations were performed with the observed reflections [$I > 2\sigma(I)$] with the program Olex2 crystallographic software packages except for refinement which was performed by SHELXL. Hydrogen atoms are refined using a riding model. CCDC 2262940-2262944 contain the supplementary crystallographic data (CIF files) for the copper(II) complexes (**1**-**5**).

4.4. Catalytic Oxidation of O_2/Cu(II)-complex/aldehyde system

All procedures of the catalytic oxidation reactions were carried out under O_2 atmosphere using an O_2 balloon unless otherwise noted. The reaction was started by adding aldehyde to a mixed solvent (CH_3CN/CH_2Cl_2, *v/v* = 3/2) containing a copper(II) complex and a substrate. After quenching the reaction by passing the reaction mixture through an alumina-column, products were analysed by GC-FID. All peaks of interest were identified by comparing the retention times with those of the authentic samples. The products were quantified by comparing their peak areas with that of an internal standard (nitrobenzene) using calibration curves consisting of plots of molar ratio (moles of organic compound/moles of internal standard) versus area ratio (area of organic compound/area of standard).

4.5. Catalytic Oxidation of *m*-CPBA/Cu(II) system

The reaction was started by adding *m*-CPBA to a mixed solvent (CH_3CN/CH_2Cl_2, *v/v* = 3/2) containing a copper(II) complex and a substrate under N_2. After quenching the reaction by passing the reaction mixture through an alumina-column, products were analysed by GC-FID. All peaks of interest were identified by comparing the retention times with those of the authentic samples. The products were quantified by comparing their peak areas with that of an internal standard (nitrobenzene) using calibration curves consisting of plots of molar ratio (moles of organic compound/moles of internal standard) versus area ratio (area of organic compound/area of standard).

4.6. Acyl radical trap experiment by CCl_4.

PhCHO (100 eq.) was added to an CH_3CN/CCl_4 (*v/v* = 3/2) solution (2.5 mL) of a copper(II)-complex (0.2 mM). The reaction mixture was stirred for 9 days at room temperature under N_2. After quenching the reaction by adding 1 mL of CH_3OH into the reaction mixture, products were analysed by GC-MS and GC-FID.

4.7. Oxidation of methane

The oxidation of methane was conducted under pressurized conditions by methane/oxygen mixture gas in a high-pressure reactor. After quenching the reaction by silica-column, products were analysed by using GC-MS. All peaks of interest were identified by comparing the retention times and mass spectra with those of the authentic samples. The products were quantified by comparing their peak areas with that of an internal standard (nitrobenzene) using a calibration curve consisting of a plot of mole ratio (moles of organic compound/moles of internal standard) versus area ratio (area of organic compound/area of internal standard).

Author contributions

S.I. conceived the idea and designed the project. K.Y. and R.K. performed most of the experiments. H.S. contributed to X-ray crystallographic analysis. Y.M. was involved in the discussion of reaction mechanism. S.I. and K.Y. wrote the manuscript. All the authors commented on the final draft of the manuscript and contributed to the analysis and interpretation of the data.

Conflicts of interest

There are no conflicts to declare.

Acknowledgements

This work was supported by JST-CREST (JPMJCR16P1 to SI).

Notes and references

1. A. E. Shilov and G. B. Shul'pin, *Chem. Rev.*, 1997, **97**, 2879-2932.
2. V. K. Ahluwalia, *Oxidation in organic synthesis*, CRC Press, Boca Raton, 2012.
3. R. H. Crabtree, *Chem. Rev.*, 1995, **95**, 987-1007.
4. N. J. Gunsalus, A. Koppaka, S. H. Park, S. M. Bischof, B. G. Hashiguchi and R. A. Periana, *Chem. Rev.*, 2017, **117**, 8521-8573.
5. P. Schwach, X. Pan and X. Bao, *Chem. Rev.*, 2017, **117**, 8497-8520.
6. V. C. C. Wang, S. Maji, P. P. Y. Chen, H. K. Lee, S. S. F. Yu and S. I. Chan, *Chem. Rev.*, 2017, **117**, 8574-8621.
7. B. E. R. Snyder, M. L. Bols, R. A. Schoonheydt, B. F. Sels and E. I. Solomon, *Chem. Rev.*, 2018, **118**, 2718-2768.
8. Y. Tang, Y. Li and F. Tao, *Chem. Soc. Rev.*, 2022, **51**, 376-423.
9. C.-M. Che, V. K.-Y. Lo, C.-Y. Zhou and J.-S. Huang, *Chem Soc. Rev.* , 2011, **40**, 1950–1975.
10. C. Tang, X. Qiu, Z. Cheng and N. Jiao, *Chem. Soc. Rev.*, 2021, **50**, 8067-8101.
11. T. Punniyamurthy, S. Velusamy and J. Iqbal, *Chem. Rev.*, 2005, **105**, 2329-2364.
12. S.-I. Murahashi, Y. Oda, T. Naota and N. Komiya, *J. Chem. Soc. Chem. Commun.*, 1993, DOI: 10.1039/C39930000139, 139-140.
13. Y. Hayashi, N. Komiya, K. Suzuki and S.-I. Murahashi, *Tetrahedron Lett.*, 2013, **54**, 2706-2709.

14. H. Sterckx, B. Morel and B. U. W. Maes, *Angew. Chem., Int. Ed.*, 2019, **58**, 7946-7970.
15. K. R. Lassila, F. J. Waller, S. E. Werkheiser and A. L. Wressell, *Tetrahedron Lett.*, 1994, **35**, 8077-8080.
16. N. Mizuno, H. Weiner and R. G. Finke, *J. Mol. Catal. A-Chem.*, 1996, **114**, 15-28.
17. W. Nam, H. J. Kim, S. H. Kim, R. Y. N. Ho and J. S. Valentine, *Inorg. Chem.*, 1996, **35**, 1045-1049.
18. B. B. Wentzel, P. A. Gosling, M. C. Feiters and R. J. M. Nolte, *J. Chem. Soc., Dalton Trans.*, 1998, DOI: 10.1039/A801175C, 2241-2246.
19. B. B. Wentzel, P. L. Alsters, M. C. Feiters and R. J. M. Nolte, *J. Org. Chem.*, 2004, **69**, 3453-3464.
20. T. Shinke, M. Itoh, T. Wada, Y. Morimoto, S. Yanagisawa, H. Sugimoto, M. Kubo and S. Itoh, *Chem. Eur. J.*, 2021, **27**, 14730-14737.
21. G. A. Russell, *J. Am. Chem. Soc.*, 1957, **79**, 3871-3877.
22. B. Maillard, K. U. Ingold and J. C. Scaiano, *J. Am. Chem. Soc.*, 1983, **105**, 5095-5099.
23. I. Garcia-Bosch and M. A. Siegler, *Angew. Chem., Int. Ed.*, 2016, **55**, 12873-12876.
24. L. Cermenati, D. Dondi, M. Fagnoni and A. Albini, *Tetrahedron*, 2003, **59**, 6409-6414.
25. H. R. Cooper and H. W. Melville, *Journal of the Chemical Society (Resumed)*, 1951, DOI: 10.1039/JR9510001984, 1984-1993.
26. H. R. Cooper and H. W. Melville, *Journal of the Chemical Society (Resumed)*, 1951, DOI: 10.1039/JR9510001994, 1994-2002.
27. W. A. Waters and C. Wickham-Jones, *Journal of the Chemical Society (Resumed)*, 1951, DOI: 10.1039/JR9510000812, 812-823.
28. J. R. McNesby and T. W. Davis, *J. Am. Chem. Soc.*, 1954, **76**, 2148-2152.
29. G. E. Zaikov, J. A. Howard and K. U. Ingold, *Can. J. Chem.*, 1969, **47**, 3017-3029.
30. M. Sankar, E. Nowicka, E. Carter, D. M. Murphy, D. W. Knight, D. Bethell and G. J. Hutchings, *Nature Communications*, 2014, **5**, 3332.
31. Y.-R. Luo, *Conprehensive Handbook of Chemical Bond Energy*, CRC Press, Boca Raton, London, New York, 2007.
32. J. Chateauneuf, J. Lusztyk and K. U. Ingold, *J. Am. Chem. Soc.*, 1988, **110**, 2877-2885.
33. C. E. H. Bawn and J. B. Williamson, *Transactions of the Faraday Society*, 1951, **47**, 721-734.
34. C. E. H. Bawn and J. E. Jolley, *Proceedings of the Royal Society of London. Series A, Mathematical and Physical Sciences*, 1956, **237**, 297-312.
35. C. H. E. Bawn, T. P. Hobin and L. Raphael, *Proceedings of the Royal Society of London. Series A, Mathematical and Physical Sciences*, 1956, **237**, 313-324.
36. C. Chatgilialoglu, D. Crich, M. Komatsu and I. Ryu, *Chem. Rev.*, 1999, **99**, 1991-2070.
37. I. V. Alabugin, L. Kuhn, M. G. Medvedev, N. V. Krivoshchapov, V. A. Vil', I. A. Yaremenko, P. Mehaffy, M. Yarie, A. O. Terent'ev and M. A. Zolfigol, *Chem. Soc. Rev.*, 2021, **50**, 10253-10345.
38. S. Winstein and F. H. Seubold, Jr., *J. Am. Chem. Soc.*, 1947, **69**, 2916-2917.
39. G.-Z. Wang, R. Shang, W.-M. Cheng and Y. Fu, *Organic Letters*, 2015, **17**, 4830-4833.
40. W. Liu, Y. Li, K. Liu and Z. Li, *J. Am. Chem. Soc.*, 2011, **133**, 10756-10759.
41. F. F. Pfaff, F. Heims, S. Kundu, S. Mebs and K. Ray, *Chem. Commun.*, 2012, **48**, 3730-3732.
42. D. D. Perrin, W. L. F. Armarego and D. R. Perrin, *Purification of Laboratory Chemicals 4th Edition*, Pergamon Press, Elmsford, NY, 4th edn., 1996.
43. J. W. Canary, Y. Wang, R. Roy Jr., J. Lawrence Que and H. Miyake, in *Inorganic Syntheses*, 1998, DOI: https://doi.org/10.1002/9780470132630.ch11, pp. 70-75.
44. K. D. Karlin, J. C. Hayes, J. P. Hutchinson, J. R. Hyde and J. Zubieta, *Inorg. Chim. Acta*, 1982, **64**, L219-L220.
45. T. Brückmann, J. Becker, C. Würtele, M. T. Seuffert, D. Heuler, K. Müller-Buschbaum, M. Weiß and S. Schindler, *J. Inorg. Biochem.*, 2021, **223**, 111544.
46. H. Wittmann, V. Raab, A. Schorm, J. Plackmeyer and J. Sundermeyer, *Eur. J. Inorg. Chem.*, 2001, **2001**, 1937-1948.
47. F. Mehlich, A. E. Roberts, M. Kerscher, P. Comba, G. A. Lawrance, C. Würtele, J. Becker and S. Schindler, *Inorg. Chim. Acta*, 2019, **486**, 742-749.
48. Y. J. Choi, K.-B. Cho, M. Kubo, T. Ogura, K. D. Karlin, J. Cho and W. Nam, *Dalton Trans.*, 2011, **40**, 2234-2241.
49. J. Wang, M. P. Schopfer, S. C. Puiu, A. A. N. Sarjeant and K. D. Karlin, *Inorg. Chem.*, 2010, **49**, 1404-1419.
50. V. V. Smirnov and J. P. Roth, *J. Am. Chem. Soc.*, 2006, **128**, 3683-3695.